Microstructure evolution during electroless copper deposition

by J. Kim S. H. Wen

D. Y. Jung R. W. Johnson

A study using transmission and scanning electron microscopy was made of the evolution of the microstructure of electroless plated Cu on activated amorphous substrates and on singlecrystal Cu grains. On amorphous substrates activated in a PdCl₂-SnCl₂ colloidal solution, Sn atoms dissolved into the plating solution concurrently with Cu deposition on the substrate during the initial stage of deposition. The very small face-centered-cubic grains of Cu-Pd solid solution agglomerated into much larger particles and later coalesced into spherical grains. As the grains grew, they developed crystallographic facets, impinged upon one another, and finally covered the entire substrate. Grains of energetically favorable crystallographic orientation selectively developed into the columnar structure. These columnar grains contained subgrains, dislocations, and twins. Remarkably different structures were observed for the Cu grown on large single-crystal grains. In this case epitaxial growth dominated the plating process. Low-surface-energy (111) Cu planes were frequently observed on plated Cu surfaces. Growth rates were a function of substrate orientation.

Copyright 1984 by International Business Machines Corporation. Copying in printed form for private use is permitted without payment of royalty provided that (1) each reproduction is done without alteration and (2) the *Journal* reference and IBM copyright notice are included on the first page. The title and abstract, but no other portions, of this paper may be copied or distributed royalty free without further permission by computer-based and other information-service systems. Permission to *republish* any other portion of this paper must be obtained from the Editor.

Introduction

Electroless copper plating is used for the fabrication of printed circuit boards (PCB), particularly those with high-aspect-ratio through-holes. One of the major concerns in this technology is the mechanical reliability of the deposited copper, which is directly related to the microstructure of the deposit. The microstructure of the deposited copper is controlled by the chemistry of the plating bath and the deposition process. This includes the activation of the substrate to initiate the autocatalytic deposition reaction as well as the nucleation and growth of the copper film. In this paper we study the microstructure evolution of the copper film during the activation and plating process and provide an understanding of the nucleation and growth phenomena.

The activation of the substrate material has been investigated by several researchers. The sensitization and activation process by double immersion in SnCl₂ and PdCl₂ solutions has been studied [1–3] and one-step activation in PdCl₂–SnCl₂ colloid solution followed by acceleration (HCl or NH₄HF₂ and others) was also investigated [4–8]. In contrast to the detailed chemical analyses presented in these researches [1–8], we studied the activation process through microstructure analysis by scanning transmission electron microscopy (STEM). This method provides information on sizes and distributions as well as chemical composition of the catalytic particles.

The nucleation and growth process determines the structural characteristics of the resultant copper deposit, which in turn determine the mechanical reliability of the PCB. Several investigations have been carried out on the effects of complexing agents and surfactants [9–12]. For example, the addition of small amounts of CN⁻ to the

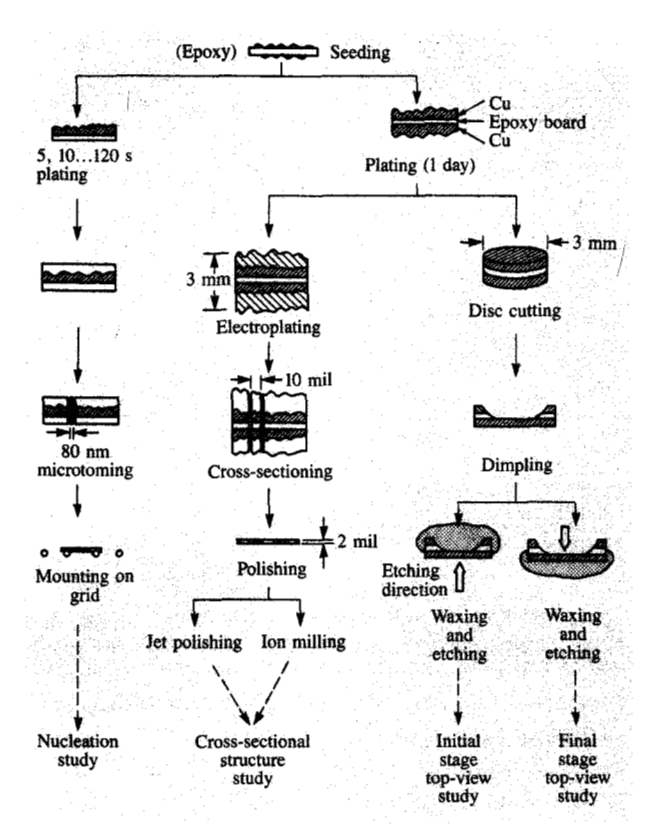


Figure 1

Various procedures for TEM specimen preparation.

plating solutions affects the mechanical properties of the copper deposit. The microstructure aspects of the copper plating were first studied by Sard [13] and Rantell [14]. Both papers concern only the early stages of copper deposition. Sard [13] proposed a three-stage development of the copper film; repeated three-dimensional nucleation at catalytic sites, followed by aggregation of the copper nuclei into particles an order of magnitude larger; and finally, recrystallization. Rantell [14] favored a dynamic coalescence model; initially deposited copper islands are mobile and coalesce as they grow larger. It was also proposed that during this dynamic process, there is deposition and dissolution of smaller islands. Through study of the microstructures, we attempt to shed light on the disagreement between these two interpretations of the nucleation stage of the copper plating process.

Little work has been done on the microstructure of plated Cu films, other than in the nucleation stage. Recently, Okinaka and Nakahara [10, 15] investigated the structure of an electroless deposited Cu film using transmission electron microscopy (TEM). Their work focused on the hydrogen voids in the electroless plated copper films. They attributed

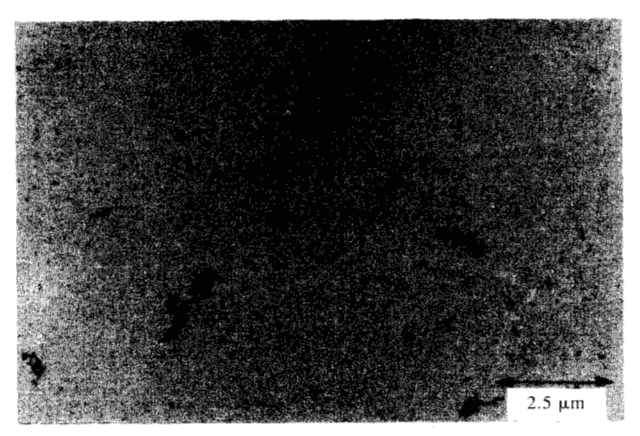


Figure 2

TEM micrograph of a $PdCl_2$ -Sn Cl_2 -activated and accelerated Si_3N_4 film.

the brittle nature of electroless copper deposit to hydrogen embrittlement. They also reported that a bath at 75°C with 2 \times 10⁻³ M NaCN yielded a deposit with void density an order of magnitude lower than the one at 60°C without cyanide.

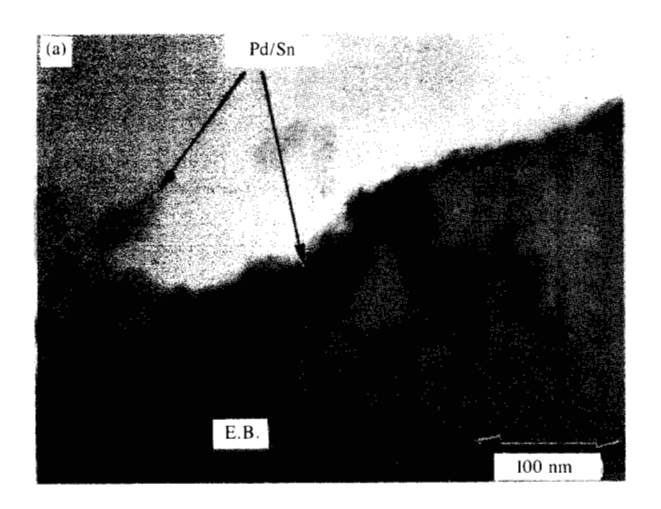
In this paper we attempt to gain further insight into the structural evolution at various stages during the electroless deposition of copper. We focus on the activation of the substrate, the nucleation and growth of copper on various activated substrates, and the structural characteristics of the resultant deposit. The effect of crystallographic orientation of the substrate on the structure of the deposit is also studied. Because the characteristics of the deposited structure change through different stages of deposition, we have devised a procedure to prepare TEM specimens for microstructure studies at various depths within a deposited film.

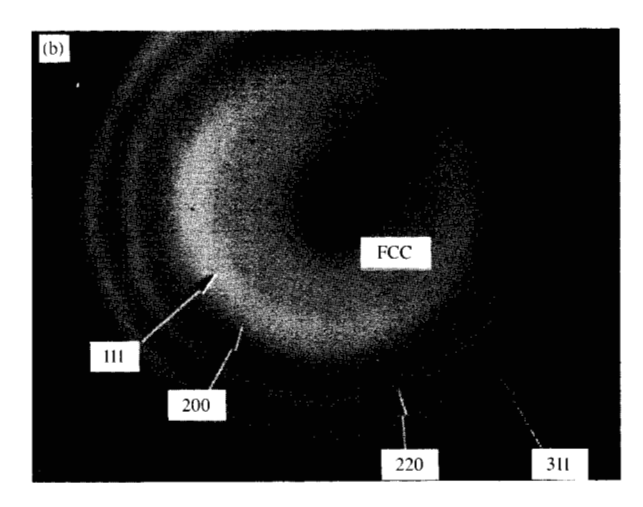
Experimental methods

The chemistry and temperature of the electroless plating bath used throughout this work were similar to those of the one (bath B) used by Okinaka and Nakahara [10], consisting of EDTA, formaldehyde, cyanide, and surfactant, except that we used a slightly lower concentration of formaldehyde and cyanide. The plating solution was frequently analyzed and the depleted components were replenished so as to maintain the concentration of Cu, formaldehyde, EDTA, CN, and surfactant. The deposition rate was monitored by weight gain using a Cu coupon with a well-defined surface area. The deposition rate used was $2.8 \pm 0.3 \ \mu m/h$.

The substrates used for the scanning electron microscopic (SEM) observations were activated epoxy, evaporated copper film, evaporated gold film, and mirror-finished polycrystalline and single crystals of copper. Activation of the substrate was done by a one-step seeding process. The

I KIM FT AL





TEM micrograph of the cross section of an activated epoxy: (a) bright field image, (b) selected area diffraction pattern.

substrate was immersed in the conventional PdCl-SnCl colloidal solution and followed by acceleration in 1 M HCl. For TEM specimen preparation, several different procedures were employed to make appropriate observations. Details for these are listed below and schematically illustrated in **Figure 1**. TEM observations were made only for the deposit on PdCl-SnCl-activated substrates.

• Initiation stage

Two methods were used to study the activation of the substrate and the initiation of the Cu deposition by TEM; the top view through an electron-transparent substrate and a side view through a cross-sectioned coupon. For the top-view observation, an electron-transparent and featureless Si₃N₄ thin film was used as a substrate. These Si₃N₄ thin films were activated and then deposited with electroless copper. The structures of the activated substrates and of the plated thin copper films were then studied by STEM. The purpose of these studies was to observe the distribution of the catalytic particles and the initial structure of the initially plated copper without any artifact due to sample preparation procedures. For cross-sectional studies, we used PCB epoxy as substrates. These substrates were then activated and plated. We subsequently encapsulated these samples in lowtemperature epoxy. Slices approximately 80 nm thick were made perpendicular to the activated and plated surfaces using an ultramicrotome.

• Later plating stage

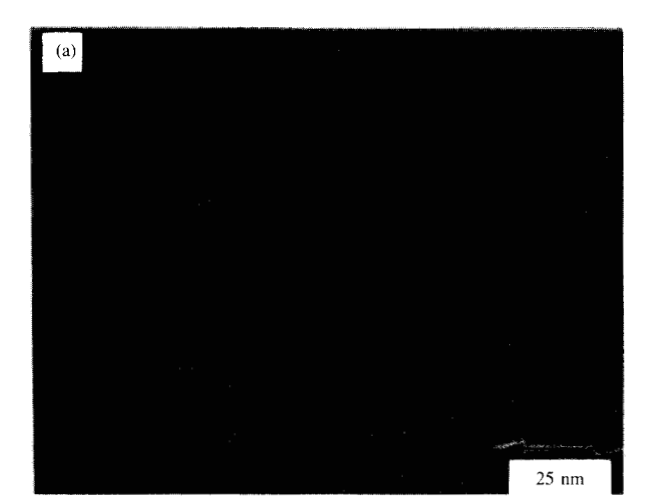
For the study of the later plating stage we used films plated to a thickness of 50 μ m. Because the plated Cu structure differs in various plating stages, and because of the thickness requirements for electron transparency (<100 nm), special

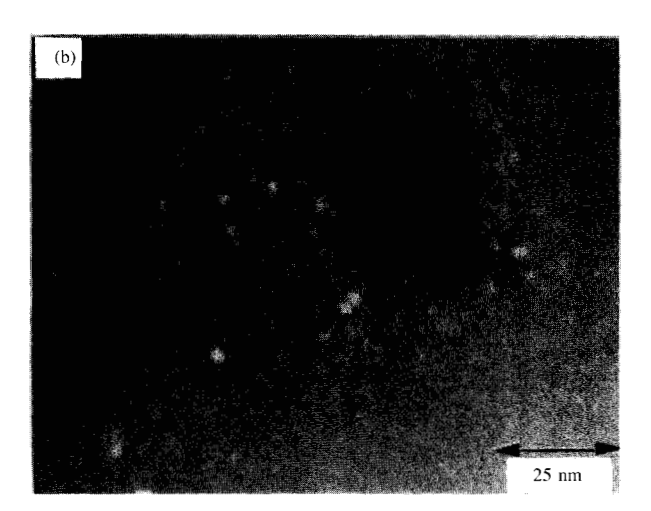
preparation procedures were required. To get the maximum amount of information, both cross-section and top-view samples were used.

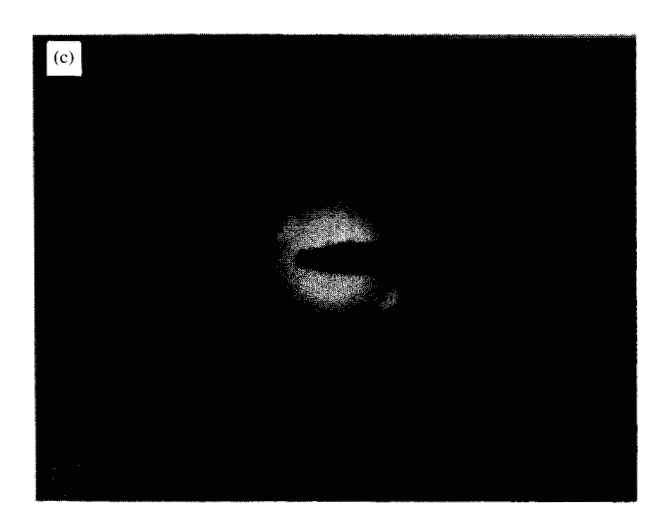
The cross-section samples are prepared as follows: The electroless plated Cu, $50~\mu m$ thick, on an epoxy coupon was then electroplated with Cu to 3 mm in total thickness and cross-sectioned into 3-mm slices. These were mechanically polished down to approximately $50~\mu m$ and further thinned to electron-transparent foils by jet-polishing in a nitric-acid-methanol (1:2) bath. Some of the $50-\mu m$ slices were ion-milled by Ar bombardment to check the possibility of artifacts introduced during specimen preparation.

The top-view samples for examining various depths within a thick deposit were prepared as follows: An epoxy coupon with 50-μm deposition of Cu was machined into 3-mm discs. These were dimpled from one side of the surface, as shown in Fig. 1. The dimpling device was set to stop immediately after the dimpler was in contact with the copper layer deposited on the opposite side. The pressure was adjusted to minimize the deformation of the deposit during dimpling. For the observation of the structure of Cu deposited at the early stage, the dimpled side was masked with thermal wax and the specimen was thinned to electron transparency by chemical polishing from the other side. The chemical polishing bath consisted of nitric, phosphoric, and acetic acids (1:1:1). TEM specimens near the top surface of the deposit were obtained by thinning from the dimpled side. TEM foils from the middle of the thickness were obtained by polishing approximately an equal amount from both sides.

The microstructure studies were done on a Philips 400T STEM equipped with energy-dispersive X-ray (EDX) capabilities for chemical analysis. The macrostructure studies were carried out on an Amray 1200B SEM.







TEM micrographs of a specimen immersed for 10 s in the plating bath: (a) BF image, (b) DF image with the aperture on (111) and (200) rings, (c) electron diffraction pattern with a convergent beam.

Results and discussion

■ Initiation stage

Figure 2 shows the distribution of Pd/Sn catalytic particles deposited on a Si₃N₄ substrate after being activated in the PdCl₂-SnCl₂ colloidal solution. The general distribution of particles and their sizes are relatively uniform from one field to another and from one specimen to another, although local variations can be seen within one field. Some agglomeration of particles is observed, e.g., the darker area in Fig. 2. A higher-magnification cross-sectional view of the activated epoxy substrate is shown in Figure 3(a). The catalytic particles are 1 to 2 nm in diameter and are clustered into groups 20 to 50 nm in size. The clusters are uniformly distributed over the substrate surface independent of the topological features. EDX analysis shows that these particles consist of Pd, Sn, and Cl as major elements, the ratio of Pd to Sn being approximately 1.5. Selected area electron diffraction shows that the particles have a face-centeredcubic (FCC) structure, Figure 3(b). These diffused diffraction rings cause difficulty in determining an exact lattice constant, but it is estimated as ≈ 0.4 nm on average. This agrees in general with those obtained by Osaka et al. [8]. The particle size effect, the variation of Pd/Sn concentration ratios in the particles, and possible strain effects may contribute to the diffuseness of the electron diffraction rings.

Once the activated substrates were immersed in the electroless plating bath, immediate deposition of copper was observed. We saw prominent Cu peaks from the EDX spectra for the specimen held in the bath for five seconds. During this early stage of deposition, Cu deposit seemed to appear concurrently with preferential dissolution of Sn from the catalytic particles into the plating solution because the composition of the deposit was mostly of Pd and Cu rather than Pd-Cu-Sn. Figures 4(a) and 4(b) are bright and dark field images of the deposit after the activated epoxy substrate was held in the bath for ten seconds. The deposit at this stage consisted of numerous spherical particles 1-2 nm in diameter, some of them being agglomerated into much larger particles. This is clearly shown in the dark field image. Fig. 4(b). A relatively sharp ring FCC diffraction pattern was obtained from this specimen. The lattice constant was approximately 0.37 nm, which is slightly larger than that for Cu but smaller than for Pd. One or two overlapping singlecrystal diffraction patterns could be obtained by converging the electron beam to 2 nm diameter and onto one or two of the small particles of approximately 2 nm diameter, Figure 4(c). This convergent beam diffraction pattern further confirmed the structure and lattice constant of the plated particles. Since Cu is known to form a stable solid solution with Pd at any composition [16], we conclude that the deposit at this stage is a solid solution of Cu and Pd rather than separate Cu and Pd grains. The mixing of Cu and Pd atoms would be enhanced by the vacant sites created on the

catalytic particles by the loss of Sn atoms. We speculate that the initiation of the plating of copper proceeds by the replacement of Sn atoms in the Pd/Sn seeds by Cu atoms.

For the immersion times of up to a few tens of seconds, the morphology of the deposit in Fig. 4(a) was maintained but showed a higher number of small particles with more frequent agglomeration appearing on longer immersion.

• Intermediate stage

Figure 5 shows a cross section of a specimen held in the bath for 1.5 min. At this stage, the deposit shows spherical grains in the range 10–50 nm in diameter. An extensive study of specimens at various immersion times failed to observe any intermediate structure between the ones shown in Figs. 4(a) and 5. This coalescence phenomenon has also been observed in the early stages of evaporation and sputtering deposition of metallic films [17, 18]. We believe that the reduction of surface energy is the driving force for the coalescence. At this stage of deposition, the Cu grains were all spherical in shape and no dislocations or twins were found.

Figure 6 is the structure of the deposit after three minutes' immersion in the bath. Some of the grains have grown to a much larger size than others. Facets of grain boundaries start to occur instead of spherical grains. This phenomenon is due



Figure 5

TEM micrograph of the cross section of a deposit after 1.5-min immersion in the bath.



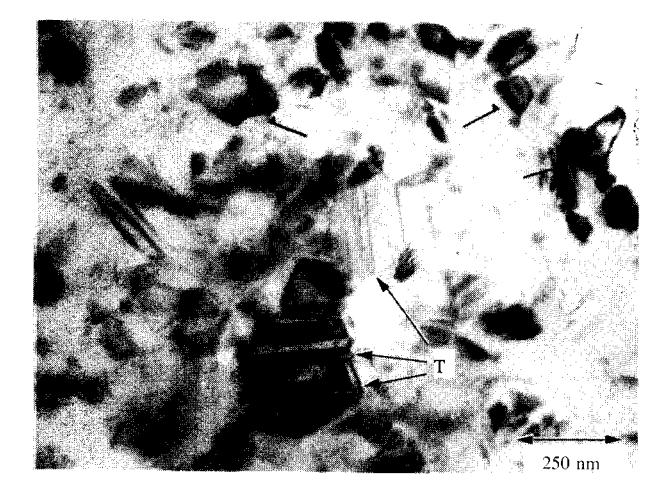
Figure 6

TEM micrograph of the deposit after 3-min immersion, Si_3N_4 substrate.

to the competitive growth of adjacent grains as well as to the lower surface energy on certain crystallographic planes that become increasingly important with grain growth.

As the grains grew further on longer immersion, the deposit showed a better continuity laterally and a structure with larger grains with facets, though showing considerable local variations in thickness of the deposit and in grain size, indicated in **Figure 7**. Many twins and dislocations were observed inside the grains and at their boundaries in **Figure 8**. This type of structure has been observed in thin films grown by evaporation and sputter deposition.

Up to the deposition time of several minutes (samples approximately a few tenths of a micrometer thick), a definite preferred orientation of the deposit was not observed; the orientation of each grain is more or less random. It appears that the Cu nucleates on the substrate randomly, and the grains subsequently coalesce, recrystallize, and grow laterally, impinging on each other before covering the whole substrate. As we show later, subsequent deposition of Cu occurs by epitaxial growth on the existing grains rather than by the nucleation, growth, and coalescence of additional Cu grains as it did in the earlier stage.



TEM micrograph of the deposit after 5-min immersion, Si_3N_4 substrate.

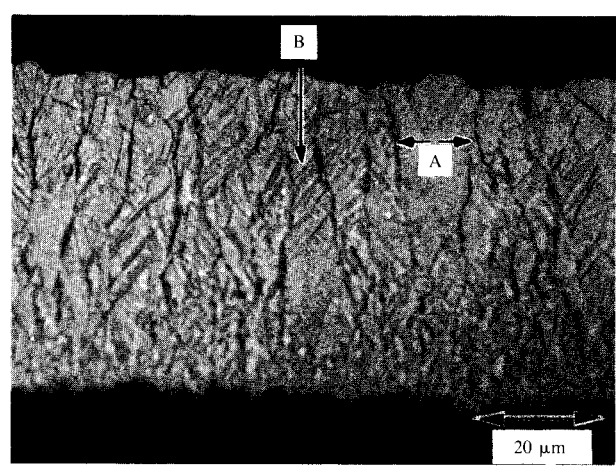


Figure 9

Optical micrograph of the cross section of a thick deposit.

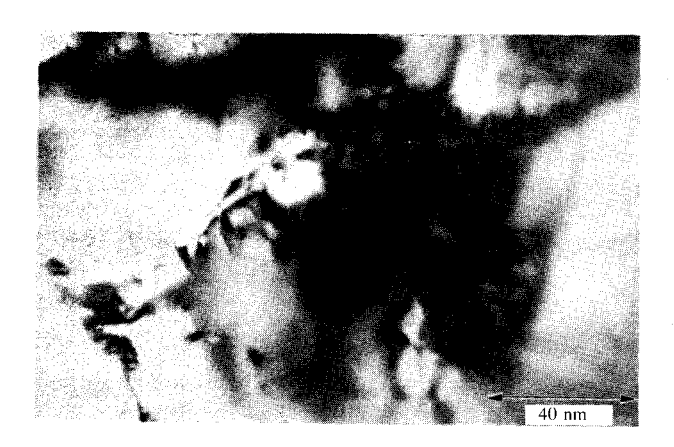


Figure 8

TEM micrograph showing the grain boundary structure of the deposit after 5-min immersion.

• Later stage growth

Figure 9 is a typical cross-sectional structure of the Cu deposited on an activated epoxy substrate. It shows that the initial layer of deposition, say up to a few micrometers, consisted of a structure of very fine grains. With further growth, the deposit developed large columnar grains oriented perpendicular to the substrate surface. The columnar grain boundaries are indicated by A in Fig. 9. The width of columnar grains is in the range of a few micrometers. Almost all the columnar grains contained subgrains (indicated as B in Fig. 9). The subgrain boundaries were generally parallel to one another within one columnar grain.

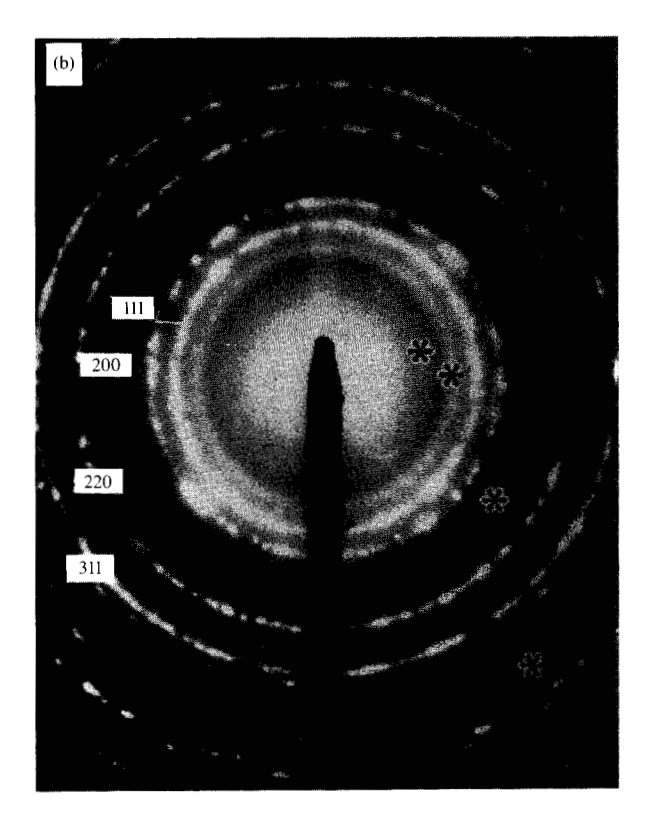
Detailed microstructure studies of the deposited copper for different deposition times were performed using the procedures outlined previously.

Figure 10(a) characterizes the region a few tenths of a micrometer away from the copper-substrate interface and represents the structure of the post-nucleation stage just prior to the formation of columnar grains. The structure at this stage shows equiaxed grains and a uniform grain size. Since the selected area diffraction pattern shows more or less continuous rings, we can conclude that the deposit at this stage, Figure 10(b), has no preferred orientation. The faint continuous rings in addition to the ones from Cu were from Cu₂O, which is probably formed during chemical polishing since the rings were absent in the sputter-thinned specimens.

The microstructure inside the columnar grains was obtained from the middle section of the 50- μ m deposit. There are subgrains with small angle boundaries inside the columnar grains. An example of these is given in Figure 11, which shows subgrain boundaries consisting of many dislocations. Exact orientations of the subgrains A, B, and C in Fig. 11 were examined by analyzing Kikuchi patterns from the grains, Figure 12. The normal direction of grain A is tilted 5.7 degrees from the (012) pole toward the (147) pole, those of B and C being tilted from the (012) pole toward the (011) pole by 2.9 and 6.4 degrees, respectively. In other words, it is 5.7 degrees between A and B and 3.5 degrees between B and C. The grain diameters were in the range of several hundred nanometers to several micrometers.

Twins were observed inside the grains, Fig. 11. All twinned structures had a common (111) twinning axis, which is typical in FCC structure crystals. Since Cu has a low stacking fault energy [19], it is not surprising to observe such a high density of twins in this material. An interesting





TEM micrograph of the specimen thinned from the surface of the thick deposit: (a) BF image, (b) diffraction pattern obtained from an area covering many grains.

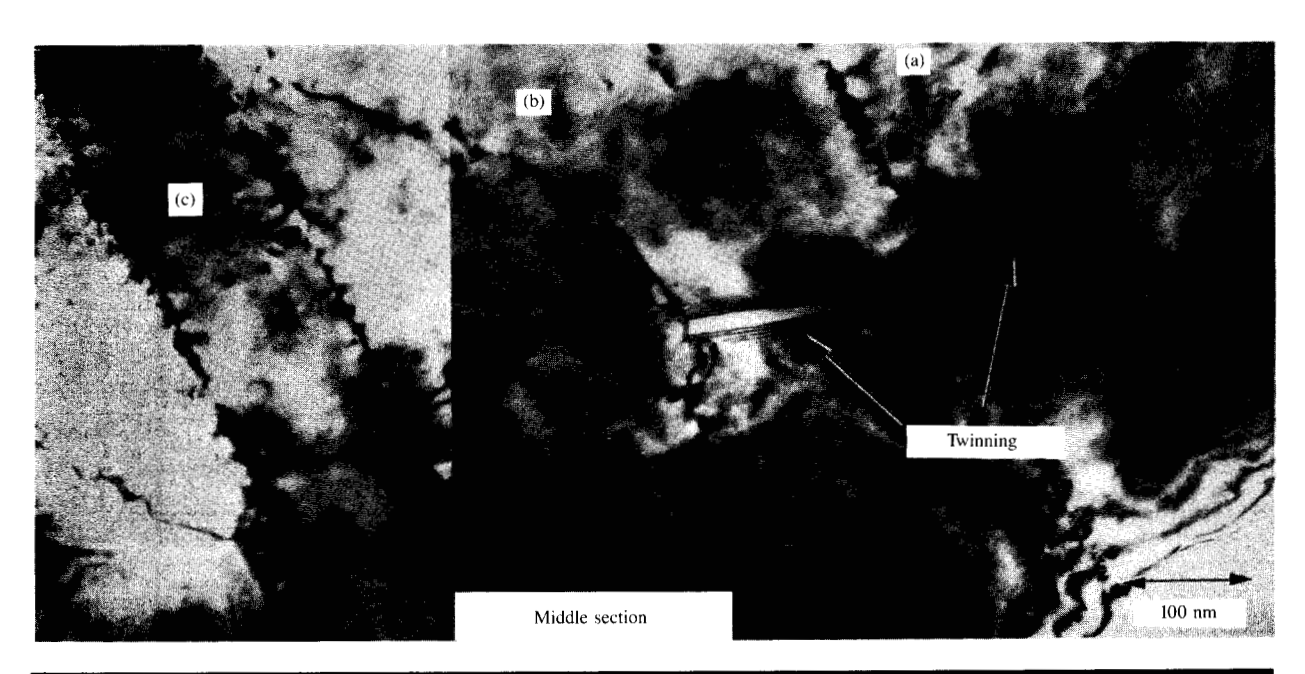
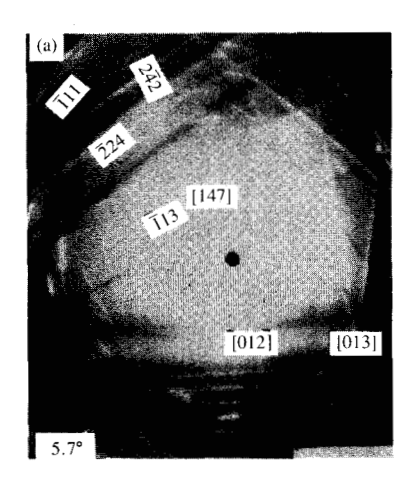
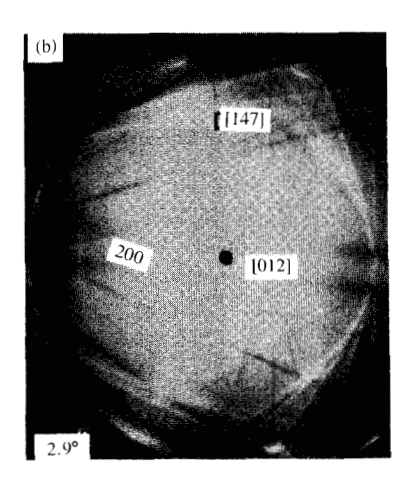


Figure 11

TEM micrograph of a specimen sampled from the middle of thickness of a thick deposit.





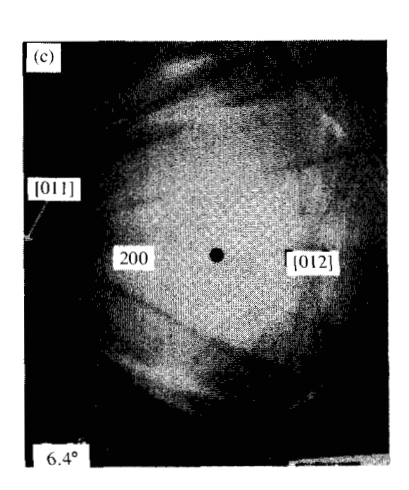
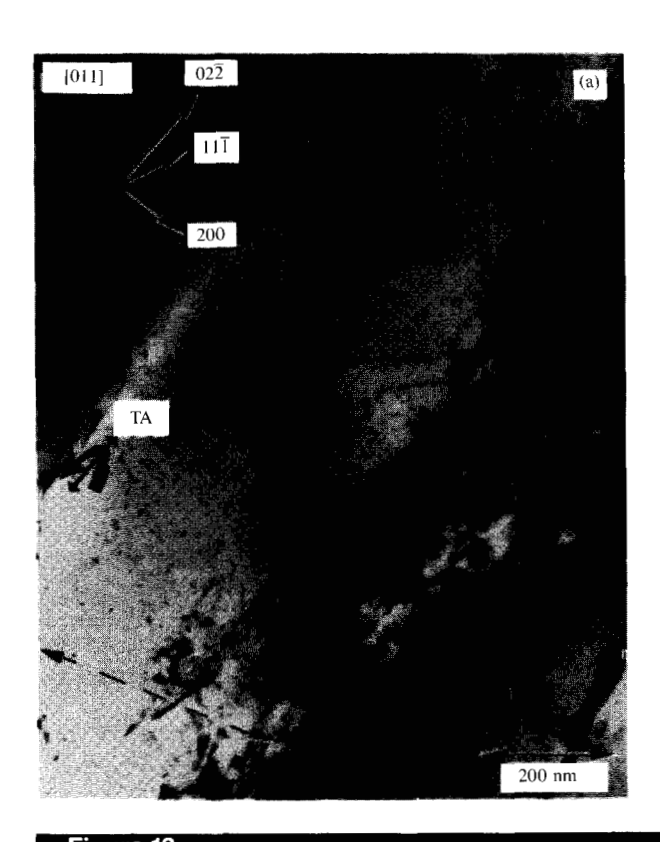


Figure 12

Kikuchi diffraction patterns of the grains A, B, and C in Fig. 11.



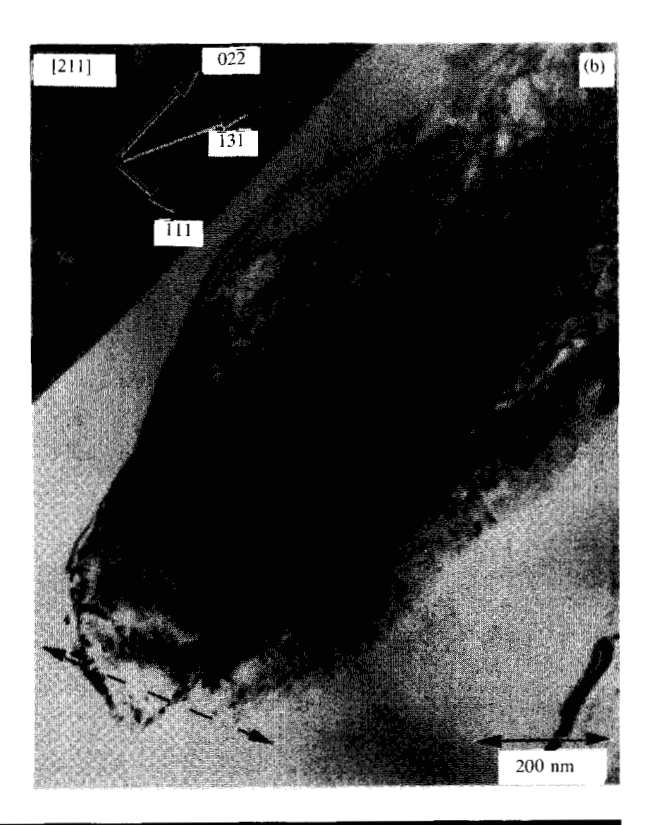


Figure 13

TEM micrographs for the cross section of a thick deposit, near the middle of the thickness. Micrograph shown in (b) corresponds to the same area as (a) but tilted. T.A. indicates the tilting axis, and the dotted line is a direction parallel to the substrate surface.

point in Fig. 11 is the coincidence of the twinning origin and the array of dislocations. One possible explanation for this

situation is that the stress field exerted from the dislocations might have been relieved by the formation of twins.

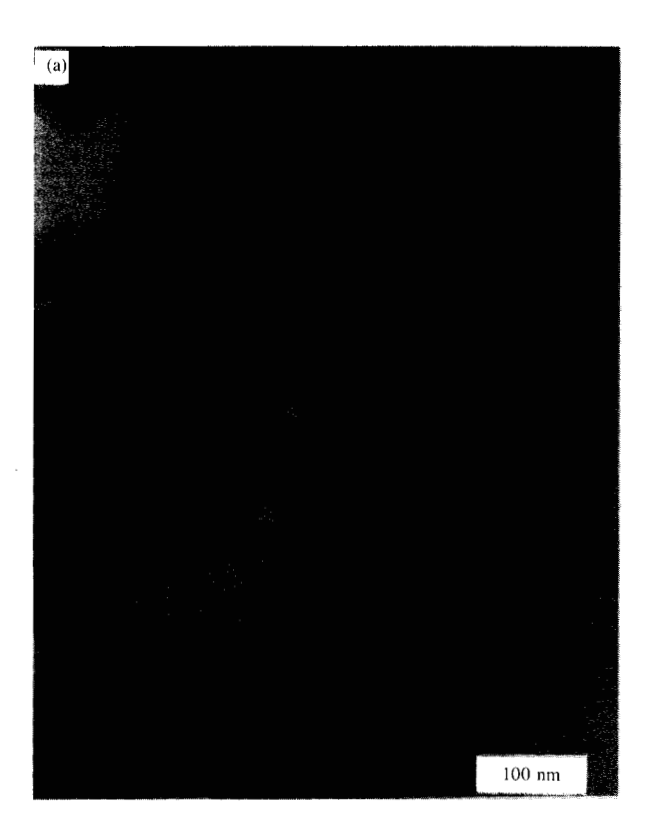




Figure 14

TEM micrographs showing voids in the foil prepared by jet-polishing. Arrow indicates voids.

In addition to the top-view studies described above, we also did cross-sectional studies in the same section, **Figure 13**. The high density of dislocations is still apparent. The longitudinal direction of the subgrains could be determined by orienting the specimen with a tilting axis parallel to the subgrain boundary. The longitudinal directions of the subgrains were determined to be parallel to the $\langle 110 \rangle$ direction. Since $\langle 110 \rangle$ is the close-packed direction for FCC materials, it is common that the subgrains parallel this direction.

Even though the subgrains have preferred parallel orientations, there is no preferred direction for the growth of columnar grains. Detailed X-ray analysis has shown random columnar grain orientations. This observation is not surprising; Junginger and Elsner [20] have shown that the preferred direction shifts from (100) to (110) or (111), depending on the chemistry of the plating bath.

We did studies of the microstructure near the top surface of 50- μ m deposit. The general characteristics were similar to the ones observed in the middle section, except for slightly larger average grain size.

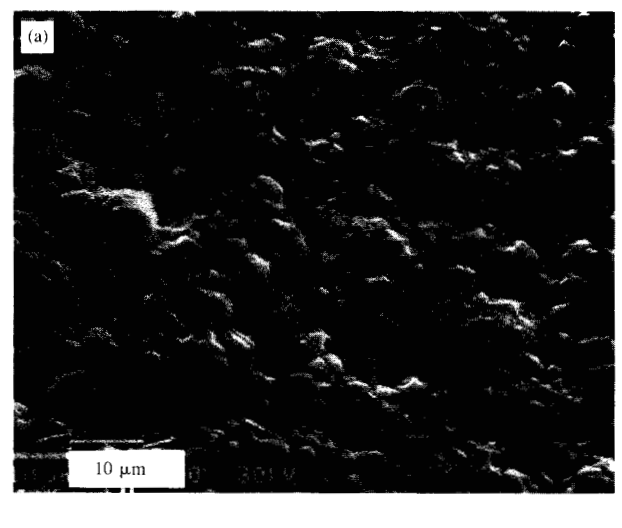
Special attention has been paid to the question of the existence of "hydrogen bubbles" described in previous works

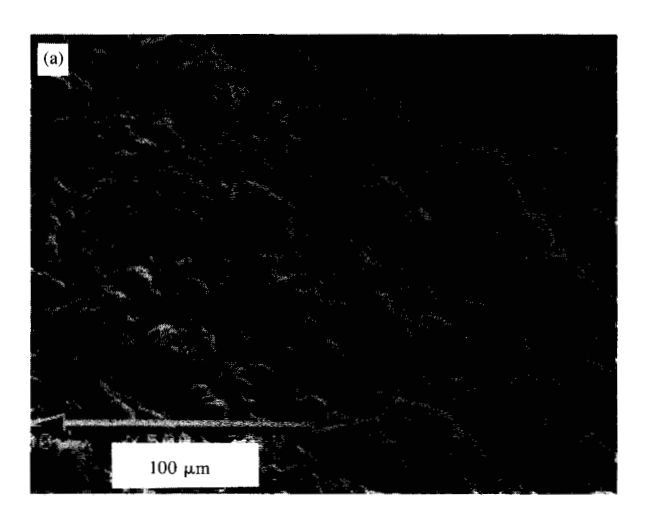
[7, 12, 21]. Small voids trapped in the bulk material can be easily observed through the Fresnel fringe by off-focusing the image. One of the well-known examples is in neutron-irradiated Mo by Eyre [22]. If there were voids, they are expected to be spherical inside grains and lenticular at the grain boundaries, due to the surface tension. **Figure 14** shows an example of the voids. The distribution of these varied from place to place and specimen to specimen. In addition, the density was much lower than in previous observations [12] (about 10¹⁴ and 10¹⁵ voids/cm³). The origin of these differences remains in question.

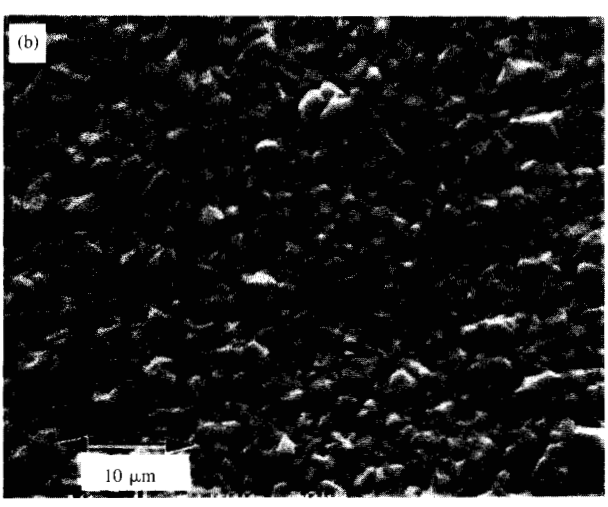
• Substrate effect on copper growth

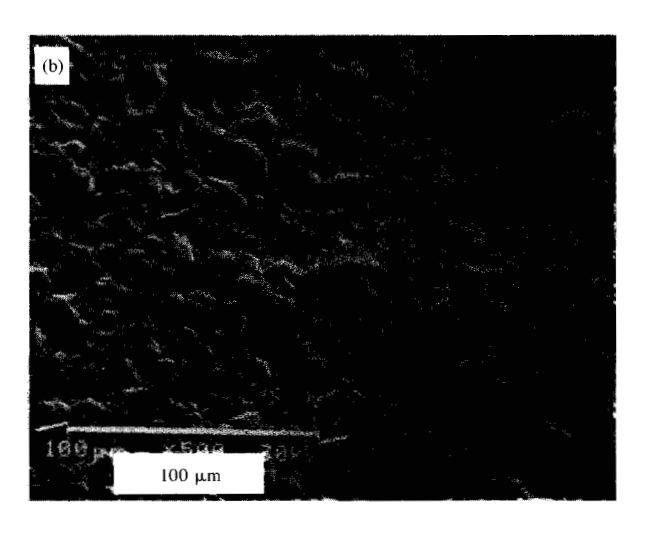
The effects of substrate materials on the nucleation and growth of copper are subjects of great interest. Nakahara and Okinaka [15] observed that a large-grained polycrystalline Cu sheet developed a structure of deposit remarkably different from the one grown on a PdCl₂-SnCl₂-activated substrate or an amorphous Pd-Cu-Si ribbon. To get further insight into this, several different substrates were deposited with electroless copper and studied with SEM.

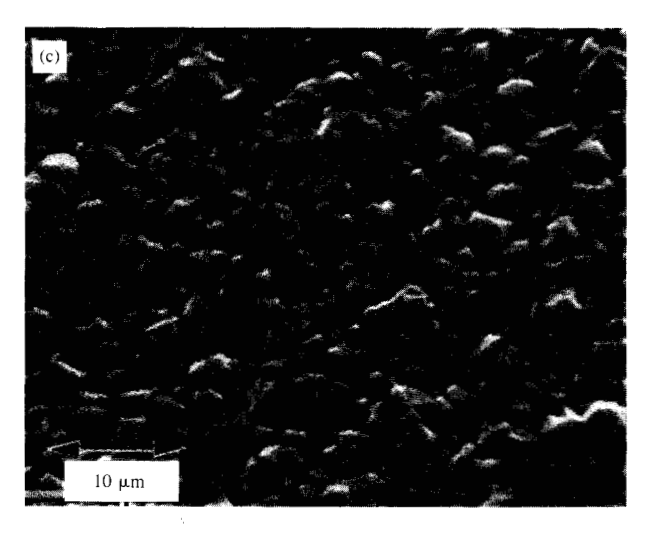
The plated structures are similar for activated amorphous substrates and very-fine-grain evaporated films. Figure 15











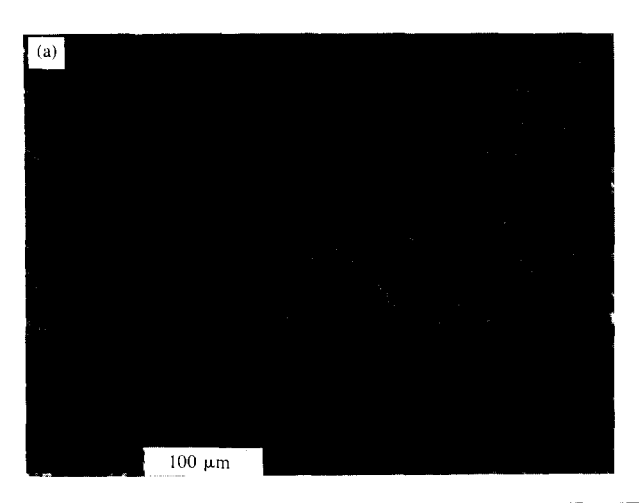
(c) 20 μm

Figure 15

Secondary electron images of the surface structure of the deposit on various substrates, after 2-h plating: (a) on an activated epoxy, (b) on an evaporated Cu film, (c) on an evaporated Au film.

Figure 16

(a) SE image of the surface of the deposit, after grown to a 50- μm film on an activated epoxy; (b) same as (a) except on an evaporated Cu film; (c) optical micrograph of the cross section of the thick deposit grown on an evaporated Cu film.



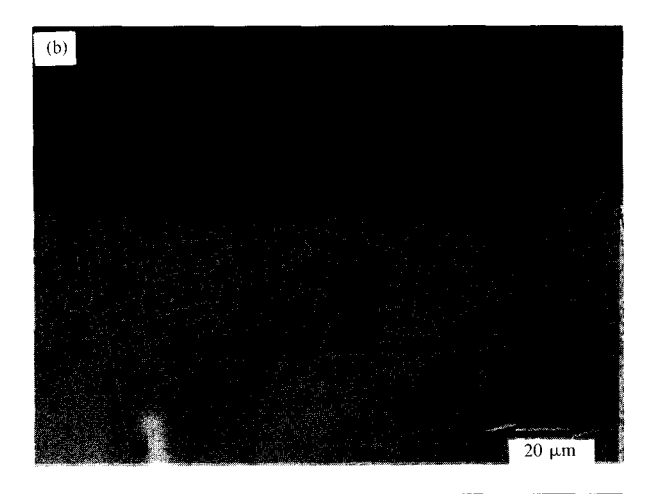


Figure 17

Structure of the deposit grown on a large-grained polycrystalline Cu: (a) SE image of the surface; (b) optical micrograph of the cross section.

shows the surface structure of the deposit grown on various substrates such as activated epoxy, Fig. 15(a), evaporated Cu film, Fig. 15(b), and evaporated Au film, Fig. 15(c), after two hours of immersion in the plating bath. The surface structure at this stage corresponds to a few micrometers from the copper substrate interface in Fig. 9, i.e., the fine equiaxed grain zone. Very little difference was found among these substrates. It is noted that the rougher surface in Fig. 15(a) is due to the original roughness of the substrate rather than to the consequence of Cu deposition.

No difference has been found with further deposition. The cross-sectional Cu structure on the evaporated film, Figure 16(c), is essentially identical to that on the activated epoxy, Fig. 9. Furthermore, the surface structure of $50-\mu m$ deposits is indistinguishable between the evaporated Cu, Figure 16(b), and $PdCl_2$ -SnCl₂-activated substrates, Figure 16(a).

However, when electroless Cu is grown on a Cu substrate with large grains, remarkably different surface and internal structures are observed, **Figure 17**. There are numerous pits bounded with four (111) surfaces, intercepting one another along (110) directions on the top view of the deposit, Fig. 17(a). This phenomenon indicates the stability of the lowest surface energy on the close-packed plane (111) in the FCC structure. Fig. 17(b) shows that many new grains grew on a single grain substrate. By studying the crystallographic orientation of the pyramidal pits, we can conclude that Fig. 17(a) consists of three individual grains. These three grains nucleated individually and epitaxially on the same big copper grain substrate with different crystallographic variants.

The effect of the crystallographic orientation of the substrate was also studied. Figures 18(a), (b), and (c) show the surface morphology of the deposit on (111), (110), and

(100) single-crystal planes. In addition to the roughness of the surface, the deposits on (111) plane show some layered characteristics indicated by an arrow. This is because the substrate is a close-packed plane and also a preferred surface plane. Fig. 18(c) shows the structure on a (100) substrate plane. It is interesting to notice that no layered characteristics, but instead pyramids, dominate the surface. This is due to the fact that (100) is 54.7 degrees away from all four (111) surfaces symmetrically. Fig. 18(b) shows the structure grown on a (110) substrate surface. Both layered structure and four-sided cone characteristics are seen here. From these observations we can conclude that the crystallographic characteristic evolved from the substrate and the lower surface energy of the close-packed plane dominates the growth morphology.

The growth rate difference on different substrate orientations is also observed. Figure 19 shows a step on the plated surface structure across a grain boundary. This observation clearly indicates that certain crystallographic surfaces are more favorable for growth than others.

The substrate structure has profound effects on the plated Cu structure. On a Pd/Sn-activated amorphous substrate such as epoxy, Si_3N_4 , or evaporated metal film on amorphous substrate, the growth characteristics are similar, as can be seen in Figs. 9 and 16(c). The Cu grains nucleated randomly on the catalytic particles or ultrafine grains having random orientation. Therefore, there is no preferred orientation at the spherical grain stage, Fig. 5, and equiaxed facet grain stage, Fig. 15. Among these randomly oriented equiaxed facet grains, Cu preferentially chemisorbs on the surface of grains having highest chemisorption energy. The energetically favorable grains start to grow epitaxially, others are suppressed, and columnar structures start to develop.





(b)

Figure 19

An SE image illustrating the different growth rate depending on the orientation of the substrate grain. The step visible in the micrograph corresponds to the grain boundary of the large-grained substrate.

(c)
1 μm 16 508 39kV

Since the surface crystallographic structure dominates the chemisorption energy, not the bulk grain orientation, the epitaxially grown columnar grains have no specific orientation relationship to one another. As we discussed above, this is not the case for large-grain substrates. The Cu grains grow on the substrate epitaxially without the competition from many different grains. Grains with different variants may be developed due to the substrate symmetries. In this case, the grains have symmetric orientation toward one another.

Figure 18

SE images of the surface of the deposit grown on single crystals, after 3½-h plating: (a) on (111) plane, (b) on (110) plane, (c) on (100) plane.

Summary

The evolution of microstructure during electroless copper deposition has been studied by scanning transmission electron microscopy and scanning electron microscopy.

The PdCl₂-SnCl₂ catalytic particles on the activated substrate, 1–2 nm in diameter, conglomerate into 20–50-nm clusters after the one-step activation process. During the early stage of deposition (five seconds), copper deposition appears to occur concurrently with dissolution of Sn from the catalytic particles. The Cu/Pd particles of 1–2-nm diameter having FCC structure form on the substrate. Similar to the seeds, these particles are agglomerated in 20–50-nm areas. After 1.5 min in the plating bath, these agglomerated areas recrystallize into spherical single-crystal grains. No crystalline defects, such as twins or dislocations, are observed at this stage. As these grains grow larger and impinge on one another, facets of grains start to develop. The grains are equiaxed and randomly oriented. Twins and dislocations are observed inside the grains and among the

boundaries. After this stage, the copper film grows into a columnar structure. No specific orientation relationship exists among the columnar grains. One columnar grain consists of many subgrains. The subgrains are separated by low angle boundaries, which are parallel to (110) directions. High-density twins and dislocations are observed. In our case, the density of voids is very low in all stages of growth.

The nucleation and growth phenomena are different for large-grain copper substrates. Substrate orientation has profound effects on growth. New grains grow epitaxially on the same substrate grain but pick up different variants. On a grain having (100) surface orientation, we observe numerous pyramidal pits bounded with four (111) surfaces intercepting each other along (110) directions. On a grain with (111) surface, a layered structure with (111) surface steps was seen. All these indicate that the close-packed plane has the lowest surface energy and therefore is most stable. The difference in growth rate for different orientations is also observed through a step across grain boundaries.

References

- B. K. W. Baylis, A. Busuttil, N. E. Hedgecock, and M. Schlesinger, "Tin(IV) Chloride Solution as a Sensitizer in Photoselective Metal Deposition," J. Electrochem. Soc. 123, 348 (1976).
- R. L. Cohen, J. F. D'Amico, and K. W. West, "Moessbauer Study of Tin(II) Sensitizer Deposits on Kapton," *J. Electrochem. Soc.* 118, 2042 (1971).
- N. Feldstein and J. A. Weiner, "Surface Characterization of Sensitized and Activated Teflon," J. Electrochem. Soc. 120, 475 (1973).
- R. L. Meek, "A Rutherford Scattering of Catalyst Systems for Electroless Cu Plating," J. Electrochem. Soc. 122, 1177 (1975).
- C. H. DeMinjer and P. F. J. v.d. Boom, "The Nucleation of SnCl-PdCl Solution of Glass Before Electroless Plating," J. Electrochem. Soc. 120, 1644 (1973).
- J. J. Grunwald, S. Gottesfeld, and D. Laser, "An Auger Spectroscopic Study of the Catalysis Process for Electroless Cu Plating," *Plat. Surf. Fin.* 68, 71 (October 1968).
- T. Osaka, H. Takematsu, and K. Nihei, "A Study on the Activation and the Acceleration by Mixed PdCl₂/SnCl₂ Catalysts for Electroless Metal Deposition," J. Electrochem. Soc. 127, 1021 (1980).
- T. Osaka, H. Nakasaku, and F. Goto, "An Electron Diffraction Study on Mixed PdCl₂/SnCl₂ Catalysts for Electroless Plating," J. Electrochem. Soc. 127, 2343 (1980).
- H. Honma and S. Mitzushima, "Applications of Ductile Electroless Copper Deposition on Printed Circuit Boards," *Jpn. Met. Finish. Tech.* 34, 290 (1983).
- Y. Okinaka and S. Nakahara, "Structure of Electroplated Hard Gold Observed by Transmission Electron Microscopy," J. Electrochem. Soc. 123, 1284 (1976).
- M. Paunovic and R. Arndt, "The Effects of Some Additives on Electroless Copper Deposition," J. Electrochem. Soc. 130, 794 (1983).
- H. Hirohata, M. Oita, and K. Honjo, "Studies on Electroless Plating of Cu," J. Met. Finish. Soc. Jpn. 21, Part 4, 485 (September 1970).
- R. Sard, "The Nucleation, Growth and Structure of Electroless Copper Deposits," J. Electrochem. Soc. 117, 864 (1970).
- A. Rantell, "The Nucleation and Growth of Electroless Plated Metal Deposited onto Plastic Substrate," *Trans. Inst. Met. Finish.* 48, 191 (1970).
- S. Nakahara and Y. Okinaka, "Microstructure and Ductility of Electroless Copper Deposits," Acta Met. 31, 713 (1983).

- R. Hultgren, R. L. Orr, P. D. Anderson, and K. K. Kelly, Selected Values of Thermodynamic Properties of Metals and Alloys, John Wiley & Sons, Inc., New York, 1963.
- D. W. Parshley, M. J. Stowell, M. H. Jacobs, and T. J. Law, "The Growth and Structure of Gold and Silver Deposits Formed by Evaporation Inside an Electron Microscope," *Phil. Mag.* 4, 127 (1964).
- C. A. Neugebauer, "Condensation, Nucleation and Growth of Thin Films," *Thin Film Technology*, L. I. Maissel and R. Glang, Eds., McGraw-Hill Book Co., Inc., New York, 1970.
- C. G. Valenzuela, "Stacking Fault Energy and Interfacial Energy of the Coherent Twin Boundaries in Copper and Brass," *Trans. Met. Soc.* 233, 1911 (1965).
- R. Junginger and G. Elsner, "Texture of Electroless (Additives) Plating," unpublished paper, IBM Boeblingen, W. Germany.
- S. Nakahara, "Microscopy in Thin Films," Thin Solid Films 64, 149 (1979).
- B. L. Eyre, Practical Electron Microscopy in Material Science, J. W. Edington, Ed., Van Nostrand Reinhold Co., New York, 1976, p. 174.

Received April 12, 1984; revised June 1, 1984

Robert W. Johnson IBM General Technology Division, P.O. Box 6, Endicott, New York 13760. Mr. Johnson joined IBM as a member of the analytical research group in Yorktown Heights, New York, in 1961. He was engaged in the design, construction, and operation of UHV analytical systems. He has since worked in the areas of Josephson technology, silicon implantation, and packaging materials surface characterization. He transferred to Endicott in 1981 and since then has been the manager of the physical analysis group. Mr. Johnson received his B.S. in chemistry from Queens College, Flushing, New York, in 1968.

Dae Young Jung IBM General Technology Division, P.O. Box 6, Endicott, New York 13760. Dr. Jung is a staff engineer in the Endicott materials engineering group. He joined IBM in Endicott in 1982, and has been involved in failure analysis of materials and in the development of advanced packaging technology. His interests are in the areas of the structure and properties of materials, surface chemistry, electrochemistry, and corrosion of metals and alloys. He received B.S. and M.S. degrees in metallurgical engineering from Seoul National University, Korea, and a Ph.D. in metallurgical engineering from the University of Illinois at Urbana-Champaign. Dr. Jung is a member of the American Society for Metals, the Electrochemical Society, and Phi Kappa Phi.

Jungihl Kim IBM Research Division, P.O. Box 218, Yorktown Heights, New York 10598. Dr. Kim received the B.S. and the M.S. degrees in physical metallurgy from Seoul National University, Korea, in 1974 and in 1976, respectively, and the Ph.D. degree in materials science from the University of California, Berkeley, in 1979. He was a research engineer at the Lawrence Berkeley Laboratory until he joined the IBM Thomas J. Watson Research Center in 1981. He has worked in packaging areas, including interface characterizations and thin film material designs. Dr. Kim is a member of the American Society of Metals, the Electrochemical Society, and the Electron Microscope Society of America.

Sheree H. Wen IBM Corporate Headquarters, 2000 Purchase St., Purchase, New York 10577. Dr. Wen is program manager for technology, Corporate Manufacturing. She joined IBM in 1979 after completing her Ph.D. in materials science and engineering at the University of California, Berkeley. Her main interests are the study of the relations between materials microstructure and chemistry and the resulting engineering properties. Dr. Wen received a First Level Invention Award in 1984. She is the recipient of the Robert Lansing Hardy Gold Medal for young materials scientist of the year, 1979, from the American Institute of Mining, Metallurgical, and Petroleum Engineers.